Draft version December 18, 2023
Typeset using LaTeX **preprint2** style in AASTeX63

Low-amplitude solar-like oscillations in ε Indi A — a K5 V star with two brown dwarfs

Mia S. Lundkvist,[1] Hans Kjeldsen,[1,2] Timothy R. Bedding,[3]
Mark J. McCaughrean,[4] R. Paul Butler,[5] Ditte Slumstrup,[6,7]
Tiago L. Campante,[8,9] Conny Aerts,[10] Torben Arentoft,[1] Hans Bruntt,[1]
Cátia V. Cardoso,[11] Fabien Carrier,[10] Laird M. Close,[12] João Gomes da Silva,[8]
Thomas Kallinger,[13] Robert R. King,[14,*] Yaguang Li (李亚光),[15]
Simon J. Murphy,[16] Jakob L. Rørsted,[1,2] and Dennis Stello[17]

[1]Stellar Astrophysics Centre, Department of Physics and Astronomy, Aarhus University, 8000 Aarhus C, Denmark
[2]Aarhus Space Centre (SpaCe), Department of Physics and Astronomy, Aarhus University, Denmark
[3]Sydney Institute for Astronomy, School of Physics, University of Sydney NSW 2006, Australia
[4]European Space Agency, ESTEC, Postbus 299, 2200 AG Noordwijk, The Netherlands
[5]Earth and Planets Laboratory, Carnegie Institution for Science, 5241 Broad Branch Road, NW, Washington, DC 20015-1305, USA
[6]European Southern Observatory, Alonso de Cordova 3107, Vitacura, Santiago, Chile
[7]Instituto de Estudios Astrofísicos, Facultad de Ingeniería y Ciencias, Universidad Diego Portales, Av. Ejército Libertador 441, Santiago, Chile
[8]Instituto de Astrofísica e Ciências do Espaço, Universidade do Porto, Rua das Estrelas, 4150-762 Porto, Portugal
[9]Departamento de Física e Astronomia, Faculdade de Ciências da Universidade do Porto, Rua do Campo Alegre, s/n, 4169-007 Porto, Portugal
[10]Institute of Astronomy, Department of Physics and Astronomy, KU Leuven, Celestijnenlaan 200 D, 3001 Leuven, Belgium
[11]Aurora Technology B.V. for ESA, ESTEC, Keplerlaan 1, 2200 AG Noordwijk, The Netherlands
[12]Department of Astronomy, University of Arizona, 933 N. Cherry Ave., Tucson, AZ 85718, USA
[13]Institute of Astrophysics, University of Vienna, 1180 Vienna, Austria
[14]School of Physics, University of Exeter, Stocker Road, Exeter EX4 4QL, UK
[15]Institute for Astronomy, University of Hawaiʻi, Honolulu, HI 96822, USA
[16]Centre for Astrophysics, University of Southern Queensland, Toowoomba, QLD 4350, Australia
[17]School of Physics, University of New South Wales, Sydney, NSW 2052, Australia

ABSTRACT

We have detected solar-like oscillations in the mid K-dwarf ε Indi A, making it the coolest dwarf to have measured oscillations. We observed ε Indi A during two radial velocity campaigns, using the high-resolution spectrographs HARPS (2011) and UVES (2021). Weighting the time series, we computed the power spectra and established the detection of solar-like oscillations with a power excess located at 5265 ± 110 μHz – the highest frequency solar-like oscillations so far measured in any star. The measurement of the center of the power excess allows us to compute a stellar mass of $0.782 \pm 0.023\ M_\odot$ based on scaling relations and a known radius from interferometry. We also determine the amplitude of the peak power and note that there is a slight difference between

Corresponding author: Mia S. Lundkvist
lundkvist@phys.au.dk

the two observing campaigns, indicating a varying activity level. Overall, this work demonstrates that low-amplitude solar-like oscillations can be detected in mid-K type stars.

Keywords: stars: individual (HD 209100) – asteroseismology – techniques: radial velocities – techniques: spectroscopic

1. INTRODUCTION

Asteroseismology, the study of stellar oscillations, has flourished in recent years thanks largely to the success of the space missions CoRoT (*Convection, Rotation and planetary Transits*, Baglin et al. 2006b,a), *Kepler* (Borucki et al. 2010; Koch et al. 2010; Chaplin et al. 2011) and TESS (Transiting Exoplanet Survey Satellite Ricker et al. 2015). These satellites delivered high-quality photometric times series that are excellent for asteroseismology. However, for bright Sun-like stars, radial velocity observations with a ground-based telescope can deliver better signal-to-noise, due to the much lower stellar granulation background. This is particularly true for cool main-sequence stars, where the oscillation amplitudes are very low (Kjeldsen et al. 2008; Huber et al. 2011).

In the case of solar-like oscillations, the overall frequency pattern is governed by two so-called global asteroseismic parameters namely the large frequency separation ($\Delta\nu$) and the frequency of maximum power ($\nu_{\rm max}$). These two parameters describe the overall regularity in the frequency comb and the location of the stellar oscillations, respectively, and they are often used to determine fundamental parameters of main-sequence and red-giant stars (see reviews by Chaplin & Miglio 2013; Jackiewicz 2021).

Here, we report the detection of solar-like oscillations in the K5 V star ε Indi A (HD 209100), which is noteworthy for having a pair of brown dwarf companions. In Sect. 2 we present our radial velocity observations and the spectroscopic analysis. The analysis of the time series with respect to asteroseismology is the topic of Sect. 3, while the results are presented and discussed in Sect. 4. The conclusion follows in Sect. 5.

* Now at Met Office, UK

2. RADIAL VELOCITY OBSERVATIONS

We observed ε Indi A in two intensive radial velocity (RV) campaigns separated in time by about 10 years. The first campaign was carried out with HARPS in 2011, while a UVES campaign followed in 2021. It should be noted that ε Indi A fell in the TESS field in Sectors 1 and 27 and was observed photometrically in the 2-minute-cadence mode for ∼27 d each. It was also observed by TESS with 20-s cadence in Sector 68. However, the oscillations are not visible in any of these data, which is to be expected given their small amplitudes.

2.1. *HARPS RV data*

The data were collected over 12 nights in August 2011 with HARPS on the ESO 3.6 m telescope at La Silla Observatory, Chile. Around 40% of the time was lost due to bad weather. The median exposure time was 30 s, sometimes increased to 35 s or 40 s in poorer conditions. The exposure time was kept short due to the high expected frequency of the oscillations. The readout time between each exposure was 32 s, and hence the median sampling time was 62 s (which corresponds to a Nyquist frequency of about 8000 μHz).

For this work we used the RVs derived by Trifonov et al. (2020) as part of the correction of public HARPS data for systematic errors. A plot of the RV time series can be found in the top panel of Fig. 1.

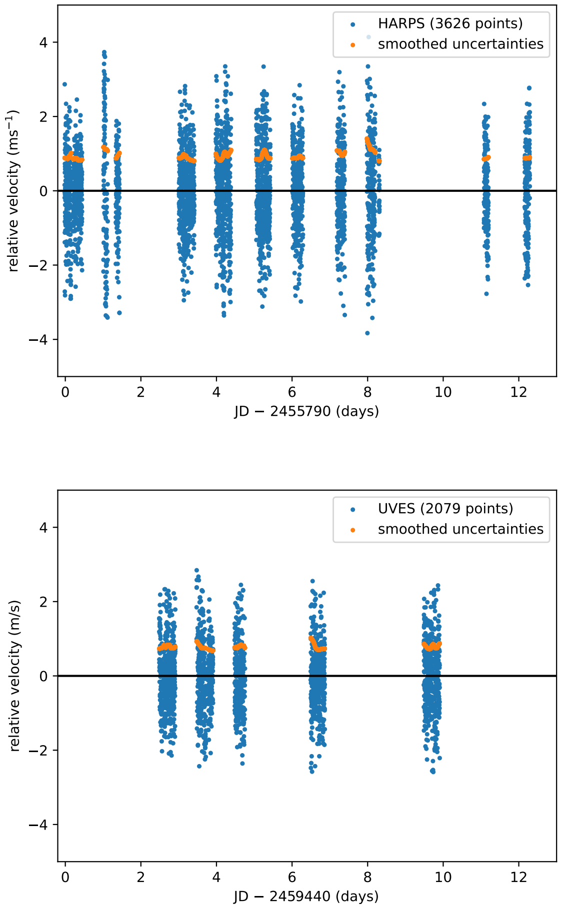

Figure 1. Radial velocity time series of ε Indi A from HARPS (August 2011) and UVES (August 2021). The orange points show the smoothed uncertainties that were measured from the scatter and used for weights when calculating the power spectra (see Sec. 3.1).

2.2. *UVES RV data*

In August 2021 we observed ε Indi A during 6 non-consecutive (5+1) nights with UVES on the VLT, using the iodine cell as a wavelength reference. Again, some time was lost due to the weather (around 25%), including all of the fourth night. The median exposure time was 50 s, with a readout time between exposures of 21 s (Nyquist frequency of about 7000 μHz).

To obtain the RV time series, all the individual spectra were reduced following the method described in Butler et al. (1996, 2004). The RV time series is shown in the bottom panel of Fig. 1.

2.3. *Spectroscopic analysis*

Some spectra taken as part of the UVES campaign were also used for a spectroscopic analysis. Based on the high signal-to-noise iodine-free template spectrum of ε Indi A, we were able to derive spectroscopic values of the effective temperature, surface gravity, [Fe/H], and the alpha enhancement using a classical equivalent-width spectral analysis with the line list from Slumstrup et al. (2019). Two sets of results are presented in Table 1, with uncertainties internal to the analysis only. One set was derived keeping the surface gravity free. The other set used a fixed surface gravity of $\log g = 4.6$, calculated using mass and radius from Demory et al. (2009). The auxiliary program ABUNDANCE within the SPECTRUM software (Gray & Corbally 1994) was used to determine the atmospheric parameters under the assumption of LTE, using ATLAS9 models (Castelli & Kurucz 2003) and solar abundances from Grevesse & Sauval (1998). We used astrophysical oscillator strengths, with the $\log gf$ values for each absorption line adjusted to yield the solar elemental abundances of Grevesse & Sauval (1998). The [α/Fe] in this paper is defined as $\frac{1}{4} \cdot$ ([Ca/Fe] + [Si/Fe] + [Mg/Fe] + [Ti/Fe]). We chose to use the values with the free $\log g$ for the subsequent analysis.

ε Indi A has been the subject of several previous spectroscopic analyses, dating as far back as 1980 (for an overview, visit for instance Simbad). The star is reported to be metal-poor, with a median [Fe/H] = -0.16 dex, which is in excellent agreement with our determination from the UVES spectrum. Median values of the effective temperature ($T_{\rm eff}$ = 4649 K) and surface gravity ($\log g = 4.54$) are also in agreement with our determined values. Based on abundances from the literature (Kollatschny 1980; Adibekyan et al. 2012; Delgado Mena et al.

Table 1. Atmospheric parameters derived from the spectroscopic analysis. Note that the quoted uncertainties are internal only (for the abundances; the spread ± the sensitivity to the other parameters), and g is measured in cm/s^2.

With free $\log g$	
$T_{\rm eff}$	$4700 \pm 65\,{\rm K}$
$\log g$	4.50 ± 0.07
[Fe/H]	$-0.17 \pm 0.01 \pm 0.03$
[α/Fe]	$-0.06 \pm 0.03 \pm 0.05$
With $\log g = 4.6$	
$T_{\rm eff}$	$4690 \pm 70\,{\rm K}$
[Fe/H]	$-0.13 \pm 0.01 \pm 0.03$
[α/Fe]	$-0.10 \pm 0.04 \pm 0.05$

2017; Luck 2018; Soto & Jenkins 2018; Hojjatpanah et al. 2019), it is possible to compute values of the alpha enhancement that can be compared to our value. The median value computed from the literature is [α/Fe] = 0.12 which, in combination with our value, indicates little to no alpha enhancement.

3. SEISMIC DATA ANALYSIS

3.1. *Calculation of the power spectrum*

We calculated weighted power spectra using a standard sine-wave fitting technique (see, e.g. Kjeldsen 1992; Frandsen et al. 1995; Handberg & Lund 2014). The weights were taken as the inverse of the measurement uncertainties, which we estimated as the smoothed scatter in the time series (orange points in Fig. 1). The median scatter was 76 cm/s for UVES and 78 cm/s for HARPS. The weighted power spectra for the HARPS and UVES observing runs are shown in the top two panels of Fig. 2 (blue lines).

To calculate the power spectrum of the combined HARPS and UVES data we merged them in the time domain, rather than averaging the power spectra, because this allowed us to estimate the spectral window of the combined data (see also Bedding & Kjeldsen 2022). This combined weighted power spectrum, shown in the bottom panel of Fig. 2, comprises around 70% power from HARPS and 30% power from UVES.

3.2. *Location of the power envelope and mode amplitude*

To determine the frequency of maximum oscillation power, $\nu_{\rm max}$, and to estimate the amplitude of the oscillations, we followed the method described by Kjeldsen et al. (2005, 2008). This involves the following steps: (i) remove the mode structure in the power spectrum by heavily smoothing with a Gaussian with a full-width at half maximum of 800 μHz ($\sim 4\Delta\nu$, with $\Delta\nu$ being the expected large frequency separation; orange curves in Fig. 2); (ii) convert to power density by multiplying by the effective length of the observing run (calculated as the reciprocal of the area under the spectral window in power); and (iii) fit and subtract the background noise using a linear fit (orange curves in Fig. 2). From this, $\nu_{\rm max}$ can be found as the peak position. We confirmed the determined value of $\nu_{\rm max}$ using two complementary approaches; a moving autocorrelation function (Huber et al. 2009; Verner & Roxburgh 2011; Lundkvist 2015) and the matched filter-response technique (Gilliland et al. 2011; Lundkvist 2015). Our detection is also supported by the SYD pipeline (Huber et al. 2009; Chontos et al. 2021), which yields a weak detection with consistent results.

A last step is needed to extract the mode amplitude, namely (iv) multiply by 4.09 (the effective number of modes per order) and take the square root, in order to convert to amplitude per oscillation mode.

4. RESULTS

The determined center of the power excess ($\nu_{\rm max}$) as well as the amplitude of the central radial mode (having degree $\ell = 0$) can be found for the HARPS, UVES and combined power spectra in Table 2. The main source of uncertainty for $\nu_{\rm max}$ and the peak amplitude is the

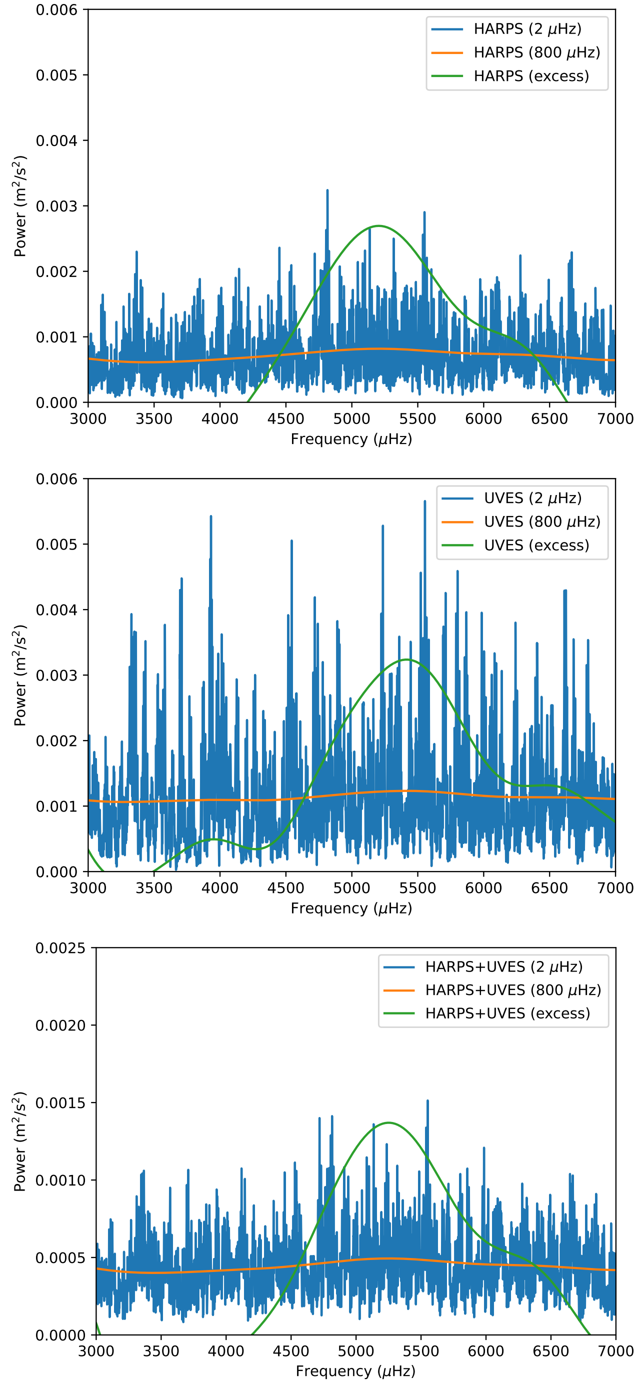

Figure 2. Power spectra of ε Indi A from HARPS (top), UVES (middle), and the combined data (bottom; note the different vertical scale). In each panel, the blue curve is the power spectrum smoothed to a width of $2\,\mu$Hz, the orange curve is smoothed by $800\,\mu$Hz, and the green curve shows the power excess after subtracting the noise (expanded vertically by a factor of 20 for visibility).

noise background. We estimated the error bars for the three excess power estimates by making simple simulations with a known input, using the same spectral window and signal-to-noise ratio as the real data. In the following, we chose to use the $\nu_{\rm max}$ from the combined power spectrum as this is based on the most data.

As an effect of the non-zero exposure time, the mode amplitudes will decrease slightly and the frequency of maximum power will shift to lower frequencies (this effect is sometimes called apodization). To understand this effect, we did simulations of the extracted peak power by creating data-sets with a known signal, but otherwise resembling those from HARPS/UVES, using an exposure time similar to the observations. From repeating this analysis 100 times we found that, to account for the non-zero exposure times, the measured peak amplitudes should be increased by 4.2% for HARPS and 12.2% for UVES, while the $\nu_{\rm max}$ values should be increased by 0.1% for HARPS and 0.4% for UVES. These corrections have been applied in Table 2.

Based on the frequency of maximum power (Table 2), the effective temperature (Table 1) as well as the computed radius from combining the distance with the measured angular diameter, we can calculate the mass of ε Indi A using the scaling relations (see e.g. Brown et al. 1991; Kjeldsen & Bedding 1995). Specifically, the mass can be found as (Stello et al. 2008; Kallinger et al. 2010):

$$\frac{M}{M_\odot} \approx \left(\frac{\nu_{\rm max}}{\nu_{\rm max,\odot}}\right)\left(\frac{R}{R_\odot}\right)^2\left(\frac{T_{\rm eff}}{T_{\rm eff,\odot}}\right)^{0.5}, \quad (1)$$

with suitable solar reference values. In this work we adopt $\nu_{\rm max,\odot} = 3090 \pm 30$ μHz (Huber et al. 2011) and $T_{\rm eff,\odot} = 5772.0 \pm 0.8$ K (Prša et al. 2016). To obtain the radius of ε Indi A we used the distance from the astrophysical parameters table of Gaia DR3 (Creevey et al. 2023): $d = 3.648^{+0.022}_{-0.009}$ pc (DISTANCE_GSPPHOT). Combin-

Table 2. Frequency of maximum oscillation power ($\nu_{\max}$) and amplitudes of the central $\ell = 0$ mode of ε Indi A (corrected for apodization).

Quantity	Symbol	Dataset	Value
Frequency of maximum power	$\nu_{\max}$	UVES	$5440 \pm 170\,\mu$Hz
		HARPS	$5210 \pm 145\,\mu$Hz
		Combined	$5265 \pm 110\,\mu$Hz
Peak amplitude	$A(\ell = 0$ at peak)	UVES	3.1 ± 0.9 cm/s
		HARPS	3.6 ± 0.7 cm/s
		Combined	3.4 ± 0.6 cm/s

ing this with the limb-darkened angular diameter of $\theta_{\rm LD} = 1.817 \pm 0.013$ mas (Rains et al. 2020) gives a radius of 0.713 ± 0.006 $R_\odot$, in excellent agreement with the value found by Rains et al. (2020). Using Eq. 1 yields a stellar mass of 0.782 ± 0.023 $M_\odot$. This is in agreement with the mass of 0.762 ± 0.038 found by Demory et al. (2009) using the interferometric radius and mass–luminosity relationship from Xia et al. (2008).

4.1. *Mode amplitude variation with the activity cycle*

We see indications of a difference between the mode amplitudes observed in the HARPS and UVES time series (see Table 2). This is not surprising as the two time series are separated by a time period of a decade, and the mode amplitudes in the Sun are known to vary over its 11-yr activity cycle (Chaplin et al. 2000; Kjeldsen et al. 2008; Kim & Chang 2022).

In fact, making use of 4293 HARPS archival data obtained for ε Indi A between 2003 and 2016, binned to 112 nights, we can place our observations in the context of the activity cycle of ε Indi A. From the HARPS archival data, we obtained the $\log R'_{\rm HK}$ values (following Gomes da Silva et al. 2018, 2021) and used those to model the activity cycle of ε Indi A. Figure 3 shows the variation of $\log R'_{\rm HK}$ phase-folded onto the estimated cycle period of ~ 2600 days. The scatter of the HARPS observations about the sinusoidal model is caused by rotational activity variations.

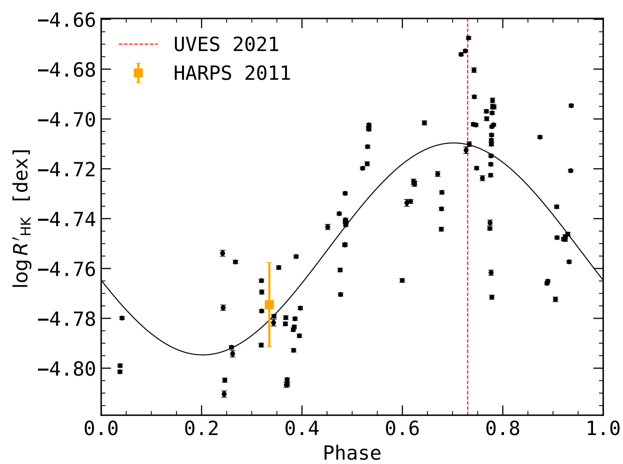

Figure 3. Phase-folded activity cycle of ε Indi A from $\log R'_{\rm HK}$. The black dots show the HARPS observations with our seismic campaign marked in yellow (error bar given by the standard deviation of the observations taken during the campaign). The red dotted line indicates the time of our UVES seismic observations, where the Ca-II H&K lines were not measured, and the solid black line represent a simple sinusoidal variation of $\log R'_{\rm HK}$ with a period of 2600 days.

As can be seen from the figure, we happened to observe ε Indi A both near the minimum (HARPS) and near the maximum (UVES) of activity. The difference between our two measurements of the oscillation amplitude is only marginally significant (Table 2) but it is noteworthy that it is consistent with expectations of an inverse correlation with activity.

5. CONCLUSION AND IMPLICATIONS

We have detected solar-like oscillations in the K5 dwarf ε Indi A. Our measured value of $\nu_{\rm max}$ of $5265 \pm 110\,\mu$Hz is the highest so far found for solar-like oscillations, surpassing Kepler-444 (K0 V; 4540 μHz; Campante et al. 2015), τ Ceti (G8 V; 4490 μHz; Teixeira et al. 2009) and α Cen B (K1 V; 4090 μHz; Kjeldsen et al. 2005). This result paves the way for detections in more early-to-mid K-dwarfs. Combining this detection with a known distance and angular diameter, we estimate the mass of ε Indi A to be $0.782 \pm 0.023\ M_{\odot}$, in agreement with literature values.

The K dwarf ε Indi A is part of a hierarchical triple system with the brown dwarfs ε Indi Ba and ε Indi Bb. This brown dwarf pair has been extensively studied (see, for example, Scholz et al. 2003; Smith et al. 2003; McCaughrean et al. 2004; Roellig et al. 2004; Mainzer et al. 2007; Reiners et al. 2007; Kasper et al. 2009; King et al. 2010; Cardoso et al. 2010; Chen et al. 2022) and the ε Indi system is valuable to put constraints on formation and evolution in the substellar regime (Joergens & Reffert 2014). With the current determined dynamical masses of $66.92 \pm 0.36\ M_{\rm Jup}$ and $53.25 \pm 0.29 M_{\rm Jup}$ for the brown dwarfs (Chen et al. 2022), as well as an accurate distance, these are among the best-characterised brown dwarfs (Chen et al. 2022). However, there is disagreement over the age of the system, with estimates spanning a range 0.39–5 Gyr (Cannon 1970; Lachaume et al. 1999; Rocha-Pinto et al. 2002; Barnes 2007; Kasper et al. 2009; King et al. 2010; Dieterich et al. 2018; Feng et al. 2019; Viswanath et al. 2021; Pathak et al. 2021; Chen et al. 2022), leaving the age to be firmly pinned down. With our detection of solar-like oscillations in ε Indi A there is now hope to do this via asteroseismology.

ACKNOWLEDGMENTS

Based on observations collected at the European Southern Observatory under ESO programmes 087.D-0511 and 105.20CY. This work was supported by a research grant (42101) from VILLUM FONDEN as well as The Independent Research Fund Denmark's Inge Lehmann program (grant agreement no.: 1131-00014B). Funding for the Stellar Astrophysics Centre was provided by The Danish National Research Foundation (grant agreement no.: DNRF106). TRB is supported by an Australian Research Council Laureate Fellowship (FL220100117). TLC is supported by Fundação para a Ciência e a Tecnologia (FCT) in the form of a work contract (CEECIND/00476/2018). J.G.S. acknowledges support from the Fundação para a Ciência e a Tecnologia (FCT) the research grants UIDB/04434/2020 & UIDP/04434/2020 and 2022.04416.PTDC. This work was cofunded by the European Union (ERC, FIERCE, 101052347). Views and opinions expressed are however those of the author(s) only and do not necessarily reflect those of the European Union or the European Research Council. Neither the European Union nor the granting authority can be held responsible for them. CA received funding from the European Research Council (ERC) under the Horizon Europe programme (Synergy Grant agreement No. 101071505: 4D-STAR). DS is supported by the Australian Research Council Discovery Grant (DP190100666). This research has made use of the SIMBAD database, operated at CDS, Strasbourg, France. This work has made use of data from the European Space Agency (ESA) mission Gaia (https://www.cosmos.esa.int/gaia), processed by the Gaia Data Processing and Analysis Consortium (DPAC, https://www.cosmos.esa.int/web/gaia/dpac/consortium). Funding for the DPAC has been provided by national institutions, in particular the institutions participating in the Gaia Multilateral Agreement.

Facilities: ESO:3.6m (HARPS), VLT:Kueyen (UVES)

REFERENCES

Adibekyan, V. Z., Sousa, S. G., Santos, N. C., et al. 2012, A&A, 545, A32, doi: 10.1051/0004-6361/201219401

Baglin, A., Michel, E., Auvergne, M., & COROT Team. 2006a, in ESA Special Publication, Vol. 624, Proceedings of SOHO 18/GONG 2006/HELAS I, Beyond the spherical Sun, ed. K. Fletcher & M. Thompson, 34

Baglin, A., Auvergne, M., Boisnard, L., et al. 2006b, in 36th COSPAR Scientific Assembly, Vol. 36, 3749

Barnes, S. A. 2007, ApJ, 669, 1167, doi: 10.1086/519295

Bedding, T. R., & Kjeldsen, H. 2022, Research Notes of the American Astronomical Society, 6, 202, doi: 10.3847/2515-5172/ac8f94

Borucki, W. J., Koch, D., Basri, G., et al. 2010, Science, 327, 977, doi: 10.1126/science.1185402

Brown, T. M., Gilliland, R. L., Noyes, R. W., & Ramsey, L. W. 1991, ApJ, 368, 599, doi: 10.1086/169725

Butler, R. P., Bedding, T. R., Kjeldsen, H., et al. 2004, ApJL, 600, L75, doi: 10.1086/381434

Butler, R. P., Marcy, G. W., Williams, E., et al. 1996, PASP, 108, 500, doi: 10.1086/133755

Campante, T. L., Barclay, T., Swift, J. J., et al. 2015, ApJ, 799, 170, doi: 10.1088/0004-637X/799/2/170

Cannon, R. D. 1970, MNRAS, 150, 111, doi: 10.1093/mnras/150.1.111

Cardoso, C. V., McCaughrean, M. J., King, R. R., et al. 2010, Highlights of Astronomy, 15, 761, doi: 10.1017/S1743921310011452

Castelli, F., & Kurucz, R. L. 2003, in IAU Symposium, Vol. 210, Modelling of Stellar Atmospheres, ed. N. Piskunov, W. W. Weiss, & D. F. Gray, 20P

Chaplin, W. J., Elsworth, Y., Isaak, G. R., Miller, B. A., & New, R. 2000, MNRAS, 313, 32, doi: 10.1046/j.1365-8711.2000.03176.x

Chaplin, W. J., & Miglio, A. 2013, ARA&A, 51, 353, doi: 10.1146/annurev-astro-082812-140938

Chaplin, W. J., Kjeldsen, H., Christensen-Dalsgaard, J., et al. 2011, Science, 332, 213, doi: 10.1126/science.1201827

Chen, M., Li, Y., Brandt, T. D., et al. 2022, AJ, 163, 288, doi: 10.3847/1538-3881/ac66d2

Chontos, A., Huber, D., Sayeed, M., & Yamsiri, P. 2021, arXiv e-prints, arXiv:2108.00582. https://arxiv.org/abs/2108.00582

Creevey, O. L., Sordo, R., Pailler, F., et al. 2023, A&A, 674, A26, doi: 10.1051/0004-6361/202243688

Delgado Mena, E., Tsantaki, M., Adibekyan, V. Z., et al. 2017, A&A, 606, A94, doi: 10.1051/0004-6361/201730535

Demory, B.-O., Ségransan, D., Forveille, T., et al. 2009, A&A, 505, 205, doi: 10.1051/0004-6361/200911976

Dieterich, S. B., Weinberger, A. J., Boss, A. P., et al. 2018, ApJ, 865, 28, doi: 10.3847/1538-4357/aadadc

Feng, F., Anglada-Escudé, G., Tuomi, M., et al. 2019, MNRAS, 490, 5002, doi: 10.1093/mnras/stz2912

Frandsen, S., Jones, A., Kjeldsen, H., et al. 1995, A&A, 301, 123

Gilliland, R. L., McCullough, P. R., Nelan, E. P., et al. 2011, ApJ, 726, 2, doi: 10.1088/0004-637X/726/1/2

Gomes da Silva, J., Figueira, P., Santos, N., & Faria, J. 2018, The Journal of Open Source Software, 3, 667, doi: 10.21105/joss.00667

Gomes da Silva, J., Santos, N. C., Adibekyan, V., et al. 2021, A&A, 646, A77, doi: 10.1051/0004-6361/202039765

Gray, R. O., & Corbally, C. J. 1994, AJ, 107, 742, doi: 10.1086/116893

Grevesse, N., & Sauval, A. J. 1998, SSRv, 85, 161, doi: 10.1023/A:1005161325181

Handberg, R., & Lund, M. N. 2014, MNRAS, 445, 2698, doi: 10.1093/mnras/stu1823

Hojjatpanah, S., Figueira, P., Santos, N. C., et al. 2019, A&A, 629, A80, doi: 10.1051/0004-6361/201834729

Huber, D., Stello, D., Bedding, T. R., et al. 2009, Communications in Asteroseismology, 160, 74. https://arxiv.org/abs/0910.2764

Huber, D., Bedding, T. R., Stello, D., et al. 2011, ApJ, 743, 143, doi: 10.1088/0004-637X/743/2/143

Jackiewicz, J. 2021, Frontiers in Astronomy and Space Sciences, 7, 102, doi: 10.3389/fspas.2020.595017

Joergens, V., & Reffert, S. 2014, Mem. Soc. Astron. Italiana, 85, 678. https://arxiv.org/abs/1407.2253

Kallinger, T., Weiss, W. W., Barban, C., et al. 2010, A&A, 509, A77, doi: 10.1051/0004-6361/200811437

Kasper, M., Burrows, A., & Brandner, W. 2009, ApJ, 695, 788, doi: 10.1088/0004-637X/695/1/788

Kim, K.-B., & Chang, H.-Y. 2022, NewA, 92, 101720, doi: 10.1016/j.newast.2021.101720

King, R. R., McCaughrean, M. J., Homeier, D., et al. 2010, A&A, 510, A99, doi: 10.1051/0004-6361/200912981

Kjeldsen, H. 1992, PhD thesis, -

Kjeldsen, H., & Bedding, T. R. 1995, A&A, 293, 87

Kjeldsen, H., Bedding, T. R., Butler, R. P., et al. 2005, ApJ, 635, 1281, doi: 10.1086/497530

Kjeldsen, H., Bedding, T. R., Arentoft, T., et al. 2008, ApJ, 682, 1370, doi: 10.1086/589142

Koch, D. G., Borucki, W. J., Basri, G., et al. 2010, ApJL, 713, L79, doi: 10.1088/2041-8205/713/2/L79

Kollatschny, W. 1980, A&A, 86, 308

Lachaume, R., Dominik, C., Lanz, T., & Habing, H. J. 1999, A&A, 348, 897

Luck, R. E. 2018, The Astronomical Journal, 155, 111, doi: 10.3847/1538-3881/aaa9b5

Lundkvist, M. S. 2015, PhD thesis, Stellar Astrophysics Centre, Aarhus University, Denmark. https://phys.au.dk/fileadmin/site_files/publikationer/phd/Mia_Sloth_Lundkvist.pdf

Mainzer, A. K., Roellig, T. L., Saumon, D., et al. 2007, ApJ, 662, 1245, doi: 10.1086/516561

McCaughrean, M. J., Close, L. M., Scholz, R.-D., et al. 2004, A&A, 413, 1029, doi: 10.1051/0004-6361:20034292

Pathak, P., Petit dit de la Roche, D. J. M., Kasper, M., et al. 2021, A&A, 652, A121, doi: 10.1051/0004-6361/202140529

Prša, A., Harmanec, P., Torres, G., et al. 2016, AJ, 152, 41, doi: 10.3847/0004-6256/152/2/41

Rains, A. D., Ireland, M. J., White, T. R., Casagrande, L., & Karovicova, I. 2020, MNRAS, 493, 2377, doi: 10.1093/mnras/staa282

Reiners, A., Homeier, D., Hauschildt, P. H., & Allard, F. 2007, A&A, 473, 245, doi: 10.1051/0004-6361:20077963

Ricker, G. R., Winn, J. N., Vanderspek, R., et al. 2015, Journal of Astronomical Telescopes, Instruments, and Systems, 1, 014003, doi: 10.1117/1.JATIS.1.1.014003

Rocha-Pinto, H. J., Castilho, B. V., & Maciel, W. J. 2002, A&A, 384, 912, doi: 10.1051/0004-6361:20011815

Roellig, T. L., Van Cleve, J. E., Sloan, G. C., et al. 2004, ApJS, 154, 418, doi: 10.1086/421978

Scholz, R.-D., McCaughrean, M. J., Lodieu, N., & Kuhlbrodt, B. 2003, A&A, 398, L29, doi: 10.1051/0004-6361:20021847

Slumstrup, D., Grundahl, F., Silva Aguirre, V., & Brogaard, K. 2019, A&A, 622, A111, doi: 10.1051/0004-6361/201833739

Smith, V. V., Tsuji, T., Hinkle, K. H., et al. 2003, ApJL, 599, L107, doi: 10.1086/381248

Soto, M. G., & Jenkins, J. S. 2018, A&A, 615, A76, doi: 10.1051/0004-6361/201731533

Stello, D., Bruntt, H., Preston, H., & Buzasi, D. 2008, ApJL, 674, L53, doi: 10.1086/528936

Teixeira, T. C., Kjeldsen, H., Bedding, T. R., et al. 2009, A&A, 494, 237, doi: 10.1051/0004-6361:200810746

Trifonov, T., Tal-Or, L., Zechmeister, M., et al. 2020, A&A, 636, A74, doi: 10.1051/0004-6361/201936686

Verner, G. A., & Roxburgh, I. W. 2011, arXiv e-prints, arXiv:1104.0631, doi: 10.48550/arXiv.1104.0631

Viswanath, G., Janson, M., Dahlqvist, C.-H., et al. 2021, A&A, 651, A89, doi: 10.1051/0004-6361/202140730

Xia, F., Ren, S., & Fu, Y. 2008, Ap&SS, 314, 51, doi: 10.1007/s10509-007-9729-8